Design and Analysis of Non-uniform Transmission Line Based Dual-Band Bandpass Filter

Mridul Gupta, Mayank Kansal, Shriram Thyagarajan, Prajjwal Singh Chauhan, and Dharmendra Kumar Upadhyay

Abstract A novel methodology for designing a microwave filter has been implemented. The designed filter is a wideband dual-band bandpass filter which has been constructed in digital domain utilizing the chain-scattering parameters for low-pass parallel coupled lines (LP-PCL), serial transmission lines and shunt connected short as well as open circuited stubs. Nature inspired metaheuristic algorithms have been utilized to approximate the magnitude response of the desired transfer function in reference to the magnitude response of ideal transfer function. The dual-band bandpass filter designs are proposed for the 2.1 and 5.2 GHz band. The configuration obtained is to be then simulated in the ADS environment utilizing RT Duroid 5880 substrate. The proposed microstrip structure is capable of covering various microwave applications, most important and common being, the WLAN operating range.

Keywords Dual-band bandpass filter · Metaheuristic optimization · Microstrip · Transmission line elements

1 Introduction

Non-uniform transmission lines have been used to design microwave dual-band bandpass filter with more precise and accurate response using Z-domain chain scattering matrices than the existing models. Specifically, the filter is constructed utilizing a synthesis method for determining the adequacy of the design technique proposed.

A novel perspective to make use of the well-developed digital signal processing techniques and optimization algorithms for designing and constructing microwave

M. Gupta (✉)
Department of Electronics and Communication Engineering, Graphic Era Deemed to be University, Dehradun 248002, India
e-mail: mri.gupta@gmail.com

M. Kansal · S. Thyagarajan · P. S. Chauhan · D. K. Upadhyay
Department of Electronics and Communication Engineering, Netaji Subhas University of Technology, Sector 3, Dwarka, New Delhi 110078, India

A. Dhawan et al. (eds.), *Advances in VLSI, Communication, and Signal Processing*,
Lecture Notes in Electrical Engineering 911,
https://doi.org/10.1007/978-981-19-2631-0_44

frequency range filters happened to be stated by Chang et al. [1]. Using the chain scattering matrices of various line sections [2], at first a prototype configuration will be proposed. The response of the prototype will be approximated to the ideal response as desired. The desired response will be achieved by adjusting the impedances of the stub using Harris Hawks algorithm for optimisation which was also used by Bao et. al for multilevel thresholding segmentation of colour image [3]. The system is synthesized using method of moments to determine the validity and usefulness of the design technique.

Standard methods for designing microwave filters generally commence with the prototype made for lumped element circuits. These elements are then transformed using Richard's transformation to stubs of same electric length [4–7]. Recently, several filters have been designed using heuristic optimization approach. Oraizi et al. [8] constructed a microwave LPF with the help of Particle Swarm Optimization, Mahata et al. [9] gave the design for fractional order digital integrators utilizing Colliding Bodies Optimization technique. Several microwave filters were designed and implemented using such algorithms by Gupta et al. [10–13].

A bandpass filter (BPF) allows frequencies to pass through within a range of onterest to pass while rejecting (attenuating) unwanted frequency components. Butterworth filter is a form of signal processing filter which is constructed to obtain a frequency response as flat as achievable in the passband. Thus, for constructing a filter with maximally flat passband, a butterworth prototype of the filter is used to approximate the filter design.

Numerous ways to design dual-band BPFs have been formulated in recent years [14–16]. The optimum method of designing a dual-band BPF is by assembling two singular band filters having dissimilar passbands [17]. One more efficient technique is to cascade a bandstop filter (BSF) and a BPF for obtaining dual-band performance [18]. A technique of designing a selectivity-enhanced Stepped impedance resonator (SIR) dual-band BPF having two open-circuited stubs is implemented in [19]. For minimizing circuit area, SIR frequencies are often utilized to form the second passband [20–23]. A dual-band BPF utilizing transversal filtering for obtaining wide stopband suppression has been implemented in [24]. In [25], a dual-band differential BPF filter has been implemented through coupling of two similar stepped impedance Ring loaded resonators (RLR). Stepped impedance ring loaded resonator was utilized by Weng et al. [26] for implementing a dual-band BPF. Cascaded structure of transversal filters and loading stubs were used to implement dual-band BPFs in [27]. Wide bandwidth using two end short-circuited SIR was achieved in the design [28]. Using the same technology, a dual-wideband has been implemented [29]. Wang et al. [30] made use of bridged-T coils was also identified to obtain dual-band BPF design with reduced size.

Bandpass filters are widely used in optics such as LIDARS, lasers, etc. These filters are applicable in WLAN, sonar, control instruments, various medical, and seismology applications. This paper is organized four sections which includes the introduction discussed in Sect. 1. Desing of dual-band BPF is explained in Sect. 2 which is followed by Sect. 3 comprising the simulations results for the proposed design. Finally, the conclusion is included as Sect. 4.

2 Design of Dual-Band BPF

Several dual-band BPFs have been designed using cascaded stuctures of wideband BPF and bandstop filter. Similar approach has been used to design dual-band BPF using serial lines, low-pass parallel coupled lines (LP-PCL) and shunt connected short as well as open circuited stubs [18]. Highly accurate and wideband design has been obtained using the proposed methodology.

2.1 Two-Port Network

There are many parameters that can be defined for the two port network namely Y-parameters, Z-parameters, ABCD parameters, S- or Scattering parameters etc. The microwave two port network is described in respect of S parameters. This is due to the fact that for a microwave system, it is impossible to measure voltage, current and phase accurately but power can be measured accurately. S-parameters are converted to chain scattering parameters or T-parameters since for a network which is made up by cascading multiple two port networks in series, the T-matrix for the overall network can be obtained by simply multiplying the individual T-matrices [1].

Given in Fig. 1 is a two-port network. Here, u(1) is the wave incident and v(1) is the wave reflected at the first port, while u(2) is the wave incident and v(2) is the wave reflected at the second port. The aforementioned waves are linked to each other by chain scattering matrices (or T-matrices) T_{ab}, a,b = 1, 2 of the network as shown:

$$\begin{pmatrix} u(1) \\ v(1) \end{pmatrix} = \begin{pmatrix} T_{11} & T_{12} \\ T_{21} & T_{22} \end{pmatrix} \begin{pmatrix} u(2) \\ v(2) \end{pmatrix} \tag{1}$$

For each of the line element under consideration, all the finite sections are assumed to have equal electrical length, i.e., $\beta l = \omega\tau$, where ω is the angular frequency and τ is propagation delay for each line element. With this, the T-parameters are converted to discrete-time domain by substituting:

$$z^{-1} = exp(-2j\beta l) \tag{2}$$

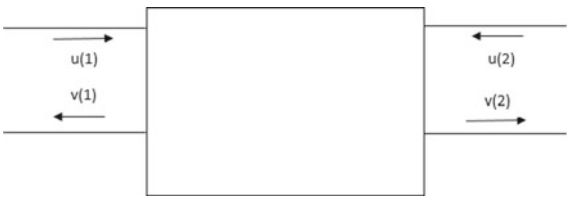

Fig. 1 Two port network device

T-matrices for the transmission line elements to be used for the proposed filter configuration are as follows:

A. *Serial transmission line* [18]:

$$T_S = \frac{1}{z^{-1/2}\left(1-\Gamma^2\right)}\begin{bmatrix} 1-\Gamma^2 z^{-1} & -\left(\Gamma-\Gamma z^{-1}\right) \\ \Gamma-\Gamma z^{-1} & -\Gamma^2+z^{-1} \end{bmatrix} \tag{3}$$

where $z = e^{jw}$, $\Gamma = (Z_1 - Z_0)/(Z_1 + Z_0)$. Here, reference characteristic impedance is Z_0 (Fig. 2).

B. *Shunt short stub* [18]:

$$T_{SSS} = \frac{1}{1-z^{-1}}\begin{bmatrix} (1+a)-(1-a)z^{-1} & a+az^{-1} \\ -a-az^{-1} & (1-a)-(1+a)z^{-1} \end{bmatrix} \tag{4}$$

where $a = Z_0/2Z_2$ (Figs. 3, 4 and 5).

III. *Shunt open stub* [18]:

$$T_{SOS} = \frac{1}{1+z^{-1}}\begin{bmatrix} (1+a)+(1-a)z^{-1} & a-az^{-1} \\ -a+az^{-1} & (1-a)+(1+a)z^{-1} \end{bmatrix} \tag{5}$$

Fig. 2 Serial transmission line configuration

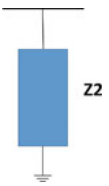

Fig. 3 Shunt short stub configuration

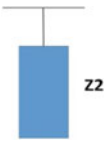

Fig. 4 Shunt open stub configuration

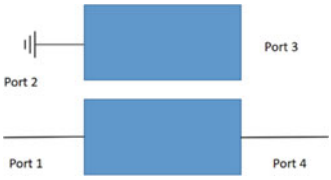

Fig. 5 LP-PCL configuration

IV. *Low-pass parallel coupled lines* [18]:

$$T_{LP-PCL} = \frac{1}{8\left(b_1^2 - b_2^2\right) Z_0 z^{-\frac{1}{2}}\left(1 - z^{-1}\right)} \begin{bmatrix} p & -s \\ r & \left(4q^2 - rs\right)/p \end{bmatrix} \tag{6}$$

where $b_1 = Z_{ev} + Z_{ov}$, $b_2 = Z_{ev} - Z_{ov}$,

$p = [4\ b_1^2 Z_0 - 2b_2^2 Z_0 + \ b_1(b_1^2 - b_2^2) + 4\ b_1 Z_0^2] + (8b_1^2 Z_0 - 12b_2^2 Z_0)\ z^{-1}$

$+[4\ b_1^2 Z_0 - 2b_2^2 Z_0 - \ b_1(b_1^2 - b_2^2) - 4\ b_1 Z_0^2]\ z^{-1}$,

$q = 4\left(b_1^2 - b_2^2\right) Z_0 z^{-\frac{1}{2}}\left(1 + z^{-1}\right)$,

$r = -2b_2^2 Z_0 + \ b_1\left(b_1^2 - b_2^2\right) - 4\ b_1 Z_0^2\big] + 4\ b_2^2 Z_0\ z^{-1}$

$+\left[-2b_2^2 Z_0 - \ b_1\left(b_1^2 - b_2^2\right) + 4\ b_1 Z_0^2\right] z^{-2}$,

$s = [2b_2^2 Z_0 + \ b_1(b_1^2 - b_2^2) - 4\ b_1 Z_0^2] - 4\ b_2^2 Z_0\ z^{-1}$

$+[2b_2^2 Z_0 - \ b_1(b_1^2 - b_2^2) + 4\ b_1 Z_0^2]\ z^{-2}$.

2.2 Location of Zeros for Multi Section Stubs

Equations (3)–(6) mention T-matrices for unit line, low-pass parallel coupled lines (LP-PCL) and shunt connected short as well as open circuited stubs in the Z-domain. Shunt connected open circuited stub provides one zero at $z = -1$ ($\Omega = \pi$) and shunt connected short circuited stub provides one zero at $= 1(\Omega = 0)$. Zero at $\Omega = \pi$ and $\Omega = 0$, improves the quality of the parameters for the stopband, while also assuring that at normalising frequency, a transmission zero is obtained. This ensures a sharp rejection at the normalising frequency which is in the stop band. Despite the fact that the serial transmission line element provides a zero at $z = 0$, the zero obtained is not found to be feasible. This predicament occurs as the delay in time is represented by $z^{-1/2}$ and for all frequencies its magnitude is one. The LP-PCL also contributes one zero at $z = -1$ which indicates that it may also be replaced by an open stub but it provides a higher stopband attenuation rate than the latter.

2.3 Design Method

The comprehensive chain scattering parameter for a cascaded sequence of multiple elements which are unit-line, low-pass parallel coupled lines and shunt connected short as well as open circuited stubs is obtained by successive multiplication of each element's chain scattering matrix, i.e.,

$$\begin{pmatrix} T_{11} & T_{12} \\ T_{21} & T_{22} \end{pmatrix} = \prod_{i=1}^{N} \begin{pmatrix} T_{11}^{(i)} & T_{12}^{(i)} \\ T_{21}^{(i)} & T_{22}^{(i)} \end{pmatrix} \tag{7}$$

where total number of stubs is denoted by N, while $T_{11}^{(i)}$, $T_{12}^{(i)}$, $T_{21}^{(i)}$, $T_{22}^{(i)}$ are the T parameters of the i^{th} stub element.

Assuming that the network comprises of P serial lines, Q short stubs and R open stubs and S LP-PCL, the T_{11} of the overall cascaded network can be given as:

$$T_{11,\,\text{network}}\,(z) = \frac{\sum_{i=1}^{Q+R+P+2S} g_i z^{-1}}{\prod_{p=1}^{P}(1-\Gamma^2)z^{-\frac{p}{2}} \prod_{r=1}^{R}(1+z^{-1}) \prod_{q=1}^{Q}(1-z^{-1}) \prod_{s=1}^{S}(1+z^{-1})z^{-\frac{s}{2}}} \tag{8}$$

where g_i is imaginary and obtained from the characteristic impedance valuess of all the line elements.

After this, for the network of comprehensive chain scattering matrix, T_{11} is calculated and transmission coefficient is obtained as:

$$H_p(z) = \frac{1}{T_{11overall}(z)} \tag{9}$$

For the line elements which form the structure, impedances are obtained through a Least Square (LS) based error function which is given by:

$$E(\omega) = \sum\nolimits_{\omega} \left[\left| H_p(\omega) \right| - |H_i(\omega)| \right]^2 \tag{10}$$

Here, $H_p(\omega)$ represents the transmission coefficient and $H_i(\omega)$ represents the ideal magnitude response.

A metaheuristic optimization algorithm named Colliding Bodies Optimization (CBO) is utilized for minimizing the error function. High level of accuracy in the magnitude response and fast convergence of rate is shown by CBO as compaired with other widely used available metaheuristic algoriths [13].

3 Simulation Results

A third order Butterworth bandpass filter is used as a prototype at normalizing frequency of 10 GHz based on which a network consisting of one shunt connected open circuit stub, one shunt connected short circuit stub and three serial lines is obtained as shown in Fig. 6. Simulated magnitude response for the proposed bandpass filter is shown in Fig. 7.

Afterwards, a third order Butterworth lowpass filter is used as a prototype at normalizing frequency of 4 GHz. When we unfold the magnitude response due to property of symmetricity the overall response for the desired 10 GHz band maps to a bandstop filter based on which a network configuration consisting of one shunt connected open circuit stub, two serial lines and one LP-PCL is obtained as shown as in Fig. 8 and the simulated response for this configuration is shown in Fig. 9.

These proposed designs are then simulated in the ADS environment. The substrate used is Rogers RT Duroid 5880 which has a relative permittivity of 2.2, substrate thickness of 20 mil and a loss tangent value of 0.0009. Equal length of $l = \lambda_o/4$ is

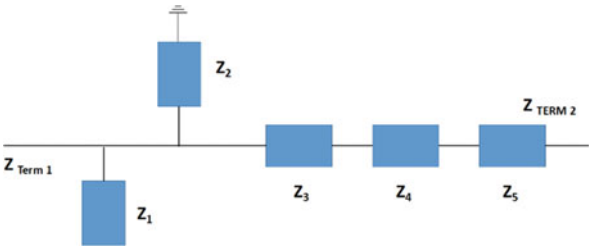

Fig. 6 Configuration of proposed bandpass filter

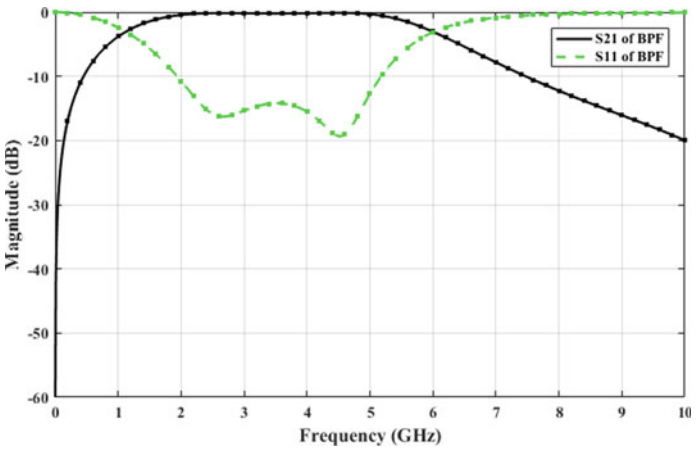

Fig. 7 Magnitude response of proposed bandpass filter

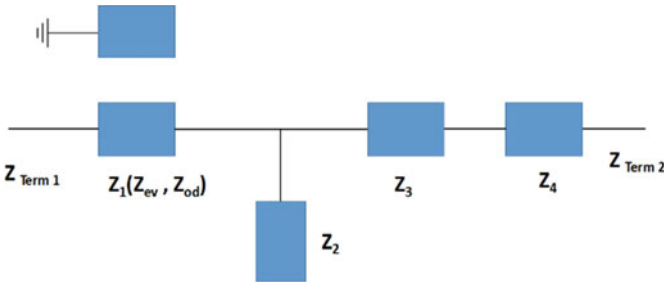

Fig. 8 Configuration of proposed bandstop filter

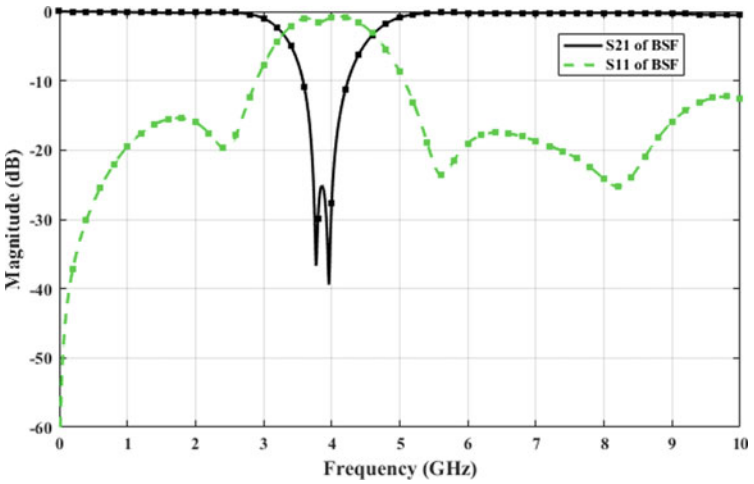

Fig. 9 Configuration of the proposed bandstop filter

considered for each line element, wherein λ_o denotes wavelength at the normalizing frequencies stated above. For the proposed designs, equivalent widths and lengths of the impedance values are calculated with the help of line calculator and further optimized in ADS using CBO algorithm and are enumerated in Tables 1 and 2.

The dual-band bandpass filter is obtained by cascading the bandpass filter and the bandstop filter designs obtained above. Figure 10 gives layout of proposed microstrip dual-band bandpass filter. The stubs have been bent at 90 degrees to make the design more compact. The dimensions of the filter are $W_1 = 1.526$ mm, $W_2 = 3.162$ mm, $W_3 = 0.288$ mm, $W_4 = 1.4$ mm, $W_5 = 3.819$ mm, $W_6 = 1.0004$ mm, $W_7 = 0.338$ mm, $W_8 = 1.4$ mm, $W_9 = 2.2$ mm, $L_1 = 4.51$ mm, $L_2 = 4.881$ mm, $L_3 = 5.882$ mm, $L_4 = 4.127$ mm, $L_5 = 4.341$ mm, $L_6 = 5.299$ mm, $L_7 = 14.959$ mm, $L_8 = 7.158$ mm, $L_9 = 7.496$ mm, $L_{10} = 6.7$ mm, $L_{11} = 6.493$ mm, $L_{12} = 8.917$ mm, $L_{13} = 6.778$ mm. 0.2 mm of diameter is used to create via holes. Total size of proposed filter is 58.3 $\times$ 15.8 mm. Simulated response for the proposed filter is shown in Fig. 11.

Table 1 Widths and lengths of line elements for the proposed bandpass configuration

Line element	Impedance (ohms)	Width (mm)	Length (mm)
Z_0	50	1.526	5.466
Z_1	29.791	3.162	5.332
Z_2	114.41	0.288	5.738
Z_3	53.203	1.385	5.484
Z_4	25.718	3.819	5.299
Z_5	61.805	1.083	5.529

Table 2 Widths and lengths of line elements for the proposed bandstop configuration

Line element	Impedance (ohms)	Width (mm)	Length (mm)
Serial Transmission Line	$Z_3 = 53.534$	1.369	13.757
	$Z_4 = 39.638$	2.139	13.555
Shunt Open Stub	$Z_2 = 107.768$	0.338	14.315
Coupled Line	$Z_{ev} = 77.735$ $Z_{od} = 45.71$	1.004	14.457
		Spacing between coupled line = 0.2 mm	

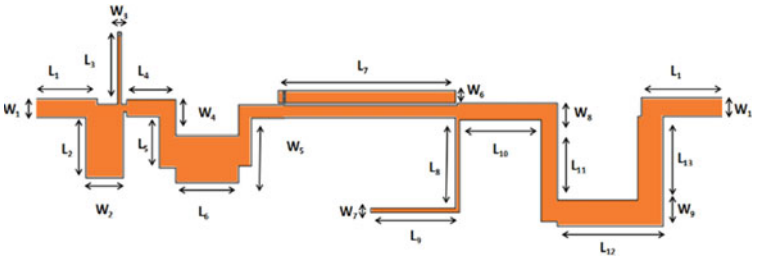

Fig. 10 Microstrip layout of proposed dual-band bandpass filter

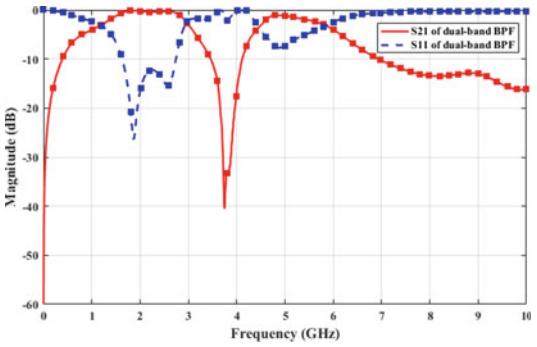

Fig. 11 Magnitude response of proposed dual-band bandpass filter

Table 3 Performance of proposed microstrip dual-band bandpass filter

Passbands	Centre frequency (GHz)	Band (3 dB) (GHz)	Bandwidth (GHz)	3 dB Fractional BW (%)	Insertion loss (dB)	Return loss (dB)
Passband 1	2.1	1.215–2.98	1.765	84	0.13	26.3
Passband 2	5.16	4.501–5.833	1.332	25.81	1.1	7.7

Performance parameters of the designed filter are shown in the Table 3. Furthermore, the comparison of proposed filter in this work with other few recently proposed dual-band bandpass filter based on various performance parameters is shown in the Table 4.

It can be observed from Table 4 that the filter design proposed in this work outperforms many other previously acclaimed dual-band bandpass filters. The size of the proposed design is also comparable and the design is easy to fabricate as it is single-layered.

Table 4 Comparison of proposed dual-band bandpass filter with its counterparts

Filter	Centre frequency (GHz)	3 dB Fractional BW (%)	Insertion loss (dB)	Return loss (dB)	Size ($\lambda_o * \lambda_o$)
Designed in [23]	2.82/3.21	5.2/5.1	1.9/1.7	21.6/16.1	2.76 * 1.3
Designed in [24]	3.78/4.82	11.3/10.6	1.38/1.82	14/33	0.16 * 0.31
Designed in [25]	1.57/2.38	9.9/6.5	1.21/1.95	19/24	–
Designed in [26]	2.6/5.8	10.4/3.6	1.1/2.15	>20	0.26 * 0.34
Designed in [27]	2.4/4	8/39	1.4/1	–	0.48 * 0.9
Designed in [30]	2.3/5.25	54/20	0.8/0.8	>20	0.3 * 0.3
Designed in [32]	2.4/5.2	51.9/23.3	0.3/0.7	22.1/20.8	0.28 * 0.2
Proposed dual-band bandpass filter	2.1/5.16	84/25.81	0.13/1.1	26.3/7.7	0.6 * 0.16

4 Conclusion

An efficient and realizable design of a dual-band bandpass filter having a wide pass-band has been provided in this work. The discrete-time (Z-domain) transfer function is obtained using the T-matrices. CBO algorithm has been used to minimize the Least Square based error function. After running multiple iterations, the optimum impedance values are achieved. The proposed design is obtained by implementing a cascaded structure comprising of a bandpass filter and a band-stop filter. Simulated response of the proposed design has wide bandwidths at 2.1/5.16 GHz which makes it suitable for various applications.

References

1. Chang, D.C., Hsue, C.W.: Design and implementation of filters using transfer functions in the Z domain. IEEE Trans. Microw. Theory Tech. **49**(5), 979–985 (2001)
2. Hsue, C.W., Tsai, Y.H., Hsu, C.C., Wu, C.Y.: Sharp rejection low-pass filter using three-section stub and Z-transform technique. IET Microwaves Antennas Propag. **4**(9), 1240–1246 (2010)
3. Bao, X., Jia, H., Lang, C.: A novel hybrid harris hawks optimization for color image multilevel thresholding segmentation. IEEE Access **7**, 76529–76546 (2019)
4. Maity, B.: Stepped impedance low pass filter using microstrip line for C-band wireless communication. In: 2016 International Conference on Computer Communication and Informatics (ICCCI), pp. 1–4. IEEE, January 2016
5. Jadhav, S.A., Misal, S.B., Mishra, A., Murugkar, A.: Designing of stepped impedance butterworth and chebyshev filters for wireless Communication. In: 2017 IEEE Applied Electromagnetics Conference (AEMC), pp. 1–2. IEEE, December 2017
6. Chen, F.C., Li, R.S., Chu, Q.X.: Ultra-wide stopband low-pass filter using multiple transmission zeros. IEEE Access **5**, 6437–6443 (2017)
7. Hayati, M., Abbasi, H., Shama, F.: Microstrip lowpass filter with ultrawide stopband and sharp roll-off. Arab. J. Sci. Eng. **39**(8), 6249–6253 (2014)
8. Oraizi, H., Esfahlan, M.S., Forati, E.: Design of stepped-impedance low pass filters with impedance matching by the particle swarm optimization and conjugate gradient method. In: 2009 European Conference on Circuit Theory and Design, pp. 639–642. IEEE, August 2009
9. Mahata, S., Saha, S.K., Kar, R., Mandal, D.: Optimal design of wideband infinite impulse response fractional order digital integrators using colliding bodies optimisation algorithm. IET Sig. Process. **10**(9), 1135–1156 (2016)
10. Gupta, M., Kansal, M., Thyagarajan, S., Chauhan, P.S., Upadhyay, D.K.: Design of an optimal microstrip butterworth low-pass filter using colliding bodies optimization. In: Dutta, D., Kar, H., Kumar, C., Bhadauria, V. (eds.) Advances in VLSI, Communication, and Signal Processing. LNEE, vol. 587, pp. 925–934. Springer, Singapore (2020). https://doi.org/10.1007/978-981-32-9775-3_82
11. Gupta, M., Upadhyay, D.K.: Design and implementation of fractional-order microwave differentiator. IET Microwaves Antennas Propag. **12**(8), 1375–1381 (2018)
12. Gupta, M., Upadhyay, D.K.: Design and implementation of second-order microwave integrator. Int. J. Electron. **107**(1), 125–140 (2020)
13. Gupta, M., Upadhyay, D.K.: Design of a coupled-line microstrip butterworth low pass filter. In: 2019 6th International Conference on Signal Processing and Integrated Networks (SPIN), pp. 939–943. IEEE, March 2019

14. Velez, P., Bonache, J., Martın, F.: Dual-band balanced bandpass filter with common-mode suppression based on electrically small planar resonators. IEEE Microwave Wirel. Compon. Lett. **26**(1), 16–18 (2015)
15. Zhu, H., Abbosh, A.M.: Single-and dual-band bandpass filters using coupled stepped-impedance resonators with embedded coupled-lines. IEEE Microwave Wirel. Compon. Lett. **26**(9), 675–677 (2016)
16. Xu, J., Chen, Z.Y., Cai, Q.H.: Design of miniaturized dual-band low-pass–bandpass and bandpass filters. IEEE Trans. Compon. Packag. Manuf. Technol. **8**(1), 132–139 (2017)
17. Chen, C.Y., Hsu, C.Y.: A simple and effective method for microstrip dual-band filters design. IEEE Microwave Wirel. Compon. Lett. **16**(5), 246–248 (2006)
18. Tsai, L.C., Hsue, C.W.: Dual-band bandpass filters using equal-length coupled-serial-shunted lines and Z-transform technique. IEEE Trans. Microw. Theory Tech. **52**(4), 1111–1117 (2004)
19. Kuo, J.T., Shih, E.: Microstrip stepped impedance resonator bandpass filter with an extended optimal rejection bandwidth. IEEE Trans. Microw. Theory Tech. **51**(5), 1554–1559 (2003)
20. Chang, S.F., Jeng, Y.H., Chen, J.L.: Dual-band step-impedance bandpass filter for multimode wireless LANs. Electron. Lett. **40**(1), 38–39 (2004)
21. Zhang, Y.P., Sun, M.: Dual-band microstrip bandpass filter using stepped-impedance resonators with new coupling schemes. IEEE Trans. Microw. Theory Tech. **54**(10), 3779–3785 (2006)
22. Weng, M.H., Wu, H.W., Su, Y.K.: Compact and low loss dual-band bandpass filter using pseudo-interdigital stepped impedance resonators for WLANs. IEEE Microwave Wirel. Compon. Lett. **17**(3), 187–189 (2007)
23. Gómez-García, R., Muñoz-Ferreras, J.M., Feng, W., Psychogiou, D.: Balanced symmetrical quasi-reflectionless single-and dual-band bandpass planar filters. IEEE Microwave Wirel. Compon. Lett. **28**(9), 798–800 (2018)
24. Wang, L.T., Xiong, Y., Gong, L., Zhang, M., Li, H., Zhao, X.J.: Design of dual-band bandpass filter with multiple transmission zeros using transversal signal interaction concepts. IEEE Microwave Wirel. Compon. Lett. **29**(1), 32–34 (2018)
25. Gómez-García, R., Yang, L., Muñoz-Ferreras, J.M., Psychogiou, D.: Selectivity-enhancement technique for stepped-impedance-resonator dual-passband filters. IEEE Microwave Wirel. Compon. Lett. **29**(7), 453–455 (2019)
26. Ren, B., Liu, H., Ma, Z., Ohira, M., Wen, P., Wang, X., Guan, X.: Compact dual-band differential bandpass filter using quadruple-mode stepped-impedance square ring loaded resonators. IEEE Access **6**, 21850–21858 (2018)
27. Weng, M.H., Lan, S.W., Chang, S.J., Yang, R.Y.: Design of dual-band bandpass filter with simultaneous narrow-and wide-bandwidth and a wide stopband. IEEE Access **7**, 147694–147703 (2019)
28. Sánchez-Soriano, M.Á., Gómez-García, R.: Sharp-rejection wide-band dual-band bandpass planar filters with broadly-separated passbands. IEEE Microwave Wirel. Compon. Lett. **25**(2), 97–99 (2014)
29. Xu, J., Ji, Y.X., Miao, C., Wu, W.: Compact single-/dual-wideband BPF using stubs loaded SIR (SsLSIR). IEEE Microwave Wirel. Compon. Lett. **23**(7), 338–340 (2013)
30. Chin, K.S., Yeh, J.H.: Dual-wideband bandpass filter using short-circuited stepped-impedance resonators. IEEE Microwave Wirel. Compon. Lett. **19**(3), 155–157 (2009)
31. Wang, Y.R., Lin, Y.S.: Size-reduction of dual-wideband bandpass filters using bridged-T coils. IEEE Access **7**, 42836–42845 (2019)
32. Liang, G.Z., Chen, F.C.: A compact dual-wideband bandpass filter based on open-/short-circuited stubs. IEEE Access **8**, 20488–20492 (2020)